New staves for old barrels: regioisomeric (1^2,2^2,3^3,4^2,5^3,6^2,7^3,8^2)-*p*-octiphenyl rods with an NMR tag†

Dawn Ronan, Damien Jeannerat, André Pinto, Naomi Sakai and Stefan Matile*

Received (in St Louis, MO, USA) 30th August 2005, Accepted 7th September 2005
First published as an Advance Article on the web 28th September 2005
DOI: 10.1039/b512276g

The usefulness of rigid-rod *p*-octiphenyls with the novel 1^2,2^2,3^3,4^2,5^3,6^2,7^3,8^2-motif as staves in rigid-rod β-barrel pores is evaluated. Comparison with the known characteristics of isomeric pores with the common 1^3,2^3,3^2,4^3,5^2,6^3,7^2,8^3-sequence indicates that the self-assembly and the supramolecular chirality of rigid-rod β-barrels are independent of the substitution pattern of the *p*-octiphenyl stave. NMR tags added at the rod termini are shown to facilitate product characterization.

1 Introduction

Conventional rigid-rod β-barrels—the only artificial β-barrels known today—are made by self-assembly of rigid-rod *p*-octiphenyl staves with peptide strands attached to the positions 1^3, 2^3, 3^2, 4^3, 5^2, 6^3, 7^2 and 8^3 (Fig. 1 and 2).[1,2] The non-planarity of the rigid-rod staves is thought to be important to preorganize cylindrical self-assembly into supramolecular oligomers and to prevent linear self-assembly into supramolecular polymers. The orthogonal orientation of neighboring amino-acid residues in a β-sheet conformation can be used to functionalize both the outer and inner surfaces of rigid-rod β-barrels in a straightforward, versatile and rational manner (Fig. 1). For the construction of synthetic multifunctional pores **1–6**, outer surface design using amino acids 1, 3 and 5 has been of use to maximize the subtle interplay between pore stability and bilayer affinity, to maximize water solubility (**4**),[3] and for ligand gating (**5**).[4] Histidines (H), arginines (R), lysines (K), and aspartates (D) have been positioned at the inner pore surface to interact with ions and molecules that move through the pore from one side of a bilayer membrane to the other.[1–5] Because of their multifunctionality, synthetic pores **1–6** turned out to be of use as supramolecular hosts,[1–8] sensors[6–8] and catalysts.[4,9]

These results identified *p*-octiphenyl β-barrels as an attractive supramolecular barrel-stave motif for the adaptable construction of synthetic ion channels and pores. For selected recent reviews of and publications in this field, please see ref. 10–18 and 19–32, respectively. The objective of this report is to explore whether or not the self-assembly of rigid-rod β-barrel pores like **1** is limited to the 1^3,2^3,3^2,4^3,5^2,6^3,7^2,8^3-substitution pattern of conventional *p*-octiphenyl staves like **7**.[1,2] To do so, isomeric *p*-octiphenyl staves **8** with a novel 1^2,2^2,3^3,4^2,5^3,6^2,7^3,8^2-motif were synthesized and characterized (Scheme 1). Nearly identical characteristics found for the nearly isomeric multifunctional pores **1** and **9** suggested that the self-assembly of rigid-rod β-barrels is independent of the relative arene substitution pattern in *p*-octiphenyl staves. Pores **1** and **9** are not exactly structural isomers because terminal methyl groups were added to the new stave. These methyls were introduced as NMR tags to facilitate the characterization of synthetic intermediates and products and to provide access to new structural insights.

2 Results and discussion

2.1 Synthesis of isomeric rigid *p*-octiphenyl rods

The isomeric, NMR-labelled *p*-octiphenyl rod **8** was prepared in eight steps from commercial biphenyls (Scheme 1). The selected route was of interest because the synthesis of the terminally activated *p*-sexiphenyl **10** in only three steps had been developed previously as an invaluable shortcut to multiply functionalized *p*-oligophenyl rods.[33] Namely, nucleophilic aromatic Sandmeyer substitution of the biphenyl bis(diazonium) salt **11** with KI gave biphenyl diiodide **12**, which was readily converted into the biphenyl boronate esters **13**. A high purity of biphenyl **13** was critical for the success of the following Suzuki coupling with excess diiodide **12**. Because of its poor solubility in the reaction mixture, *p*-sexiphenyl **10** could be accumulated, isolated and purified in up to 10% yield. Not impressive as such, this yield is much higher than the yield expected for the stepwise synthesis of *p*-sexiphenyl **10** by repeated couplings, not to mention so far unresolved problems in such a multistep exercise, such as direct terminal iodination of *p*-sexiphenyls.

Department of Organic Chemistry, University of Geneva, Geneva, Switzerland. E-mail: stefan.matile@chiorg.unige.ch; Fax: +41(0)22 379 3215; Tel: +41(0)22 379 6523

† Abbreviations. Arg, R: L-arginine; BOC: *tert*-butoxycarbonyl; CD: circular dichroism; DMF: *N*,*N*-dimethylformamide; EC50: effective c_M (monomer concentration to reach 50% pore activity); EYPC-LUVs⊃ANTS/DPX: egg yolk phosphatidylcholine (EYPC) large unilamellar vesicles (LUVs) loaded with 8-amino-1,3,6-naphthalenetrisulfonate (ANTS) and *p*-xylenebis(pyridinium) bromide (DPX); *Gla*, *G*: $-OCH_2CO-$ (H-*Gla*-OH: glycolic acid); HATU: *N*-(dimethylamino-1*H*-1,2,3-triazolo[4,5-*b*]pyridin-1-ylmethylene)-*N*-methylmethanaminium hexafluorophosphate *N*-oxide; His, H: L-histidine; IC50: inhibitory c_B (blocker concentration to reduce to 50% pore activity); ICR: internal charge repulsion; Leu, L: L-leucine; NOESY: nuclear Overhauser effect spectroscopy; Pmc: 2,2,5,7,8,-pentamethylchromane-6-sulfonyl; TEA: triethylamine; TFA: trifluoroacetic acid; Trt: trityl.

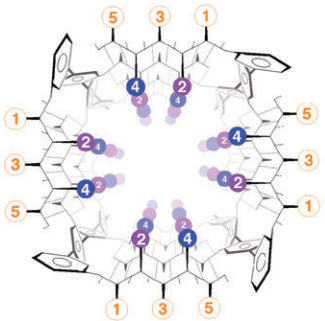

barrel	1	2	3	4	5
1	L	R	L	H	L
2	L	H	L	H	L
3	L	K	L	H	L
4	L	R	W	H	V
5	L	H	R	H	L
6	L	D	L	D	L

Fig. 1 Axial view of six previously made and characterized multifunctional rigid-rod β-barrel pores with β-sheets shown as solid (backbone) and dotted lines (hydrogen bonds) and amino-acid residues at the outer (1, 3, 5) and inner (2, 4) barrel surfaces dark on white and white on dark, respectively (single-letter abbreviations). For side views of rigid-rod β-barrel pores, see Fig. 2.

The terminal NMR tags were prepared from nitroanisol **14** following a recent report by Coleman *et al.*[34] Reduction gave amine **15**, which was subjected to Sandmeyer treatment *via* the diazonium salt to afford iodoanisol **16**.[34,35] Transformation into the pinacol boronate ester **17** prepared for the Suzuki coupling with *p*-sexiphenyl **10**. The methoxys along the scaffold of the resulting *p*-octiphenyl **18** were then cleaved with BBr_3, and the obtained octaphenol **19** was reacted with *tert*-butyl bromoacetate. Deprotection of *p*-octiphenyl **20** liberated the carboxylic acids along the rigid-rod scaffold of **21** for coupling with the N-terminus of the previously reported pentapeptide **22**.[36] Side-chain deprotection gave target rod **8** as a TFA salt.

The target molecule **8** was purified by semi-preparative RP-HPLC. HPLC chromatograms and mass spectra of isomers **7** and **8** and their protected precursors showed qualitatively

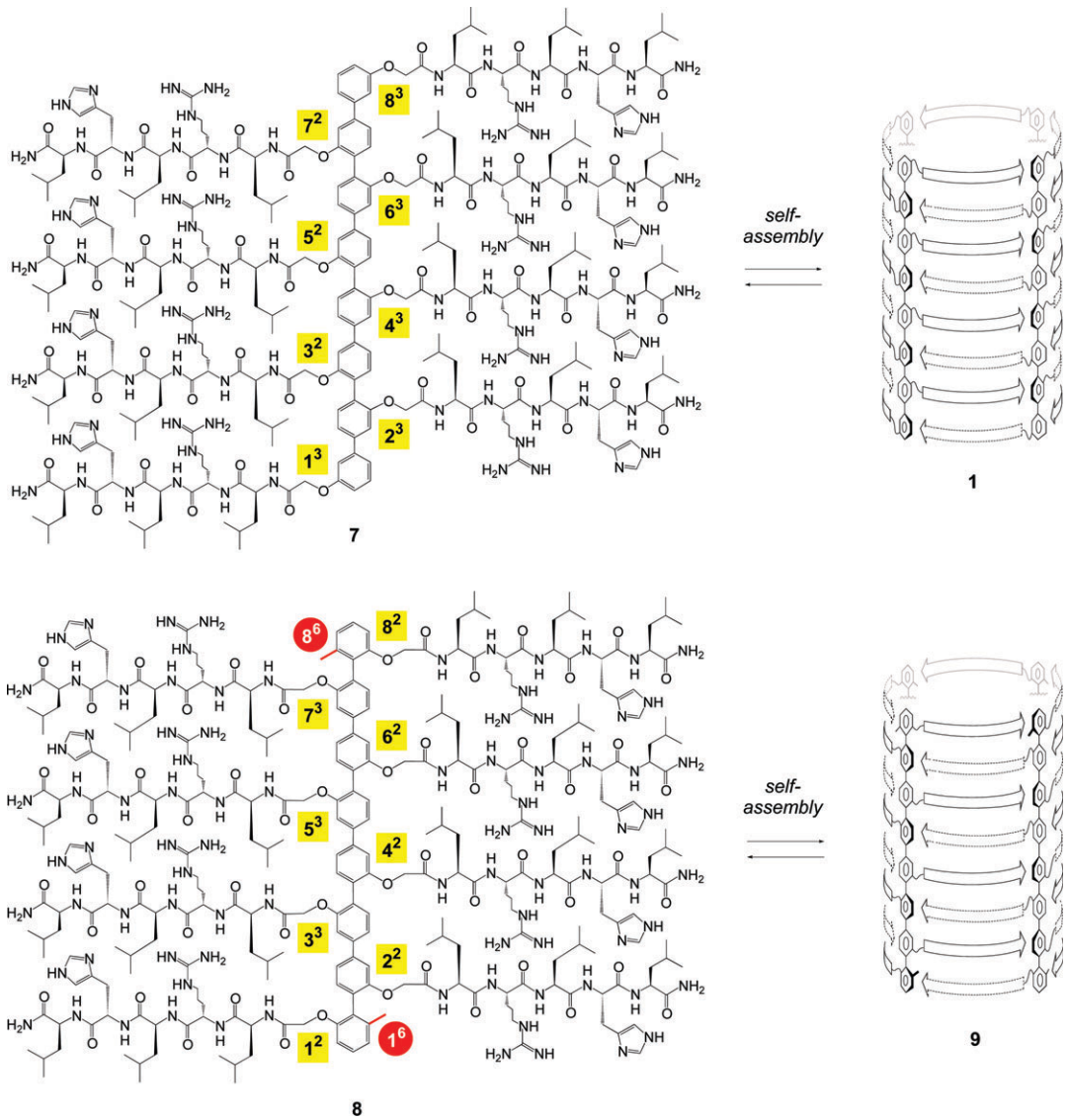

Fig. 2 Self-assembly of conventional and isomeric *p*-octiphenyl-peptide conjugates **7** and **8** into conventional and isomeric multifunctional rigid-rod β-barrel pores **1** and **9**, respectively. Amino-acid residues are shown in neutral form. Under conditions relevant for function, arginine (R) residues are expected to be fully protonated and complexed with exchangeable counteranions, mainly inorganic phosphates,[37] whereas histidine (H) residues are partially protonated below pH 6 only. Arrows represent β-sheets (N→C). For axial views of rigid-rod β-barrel pores, see Fig. 1, 6 and 8.

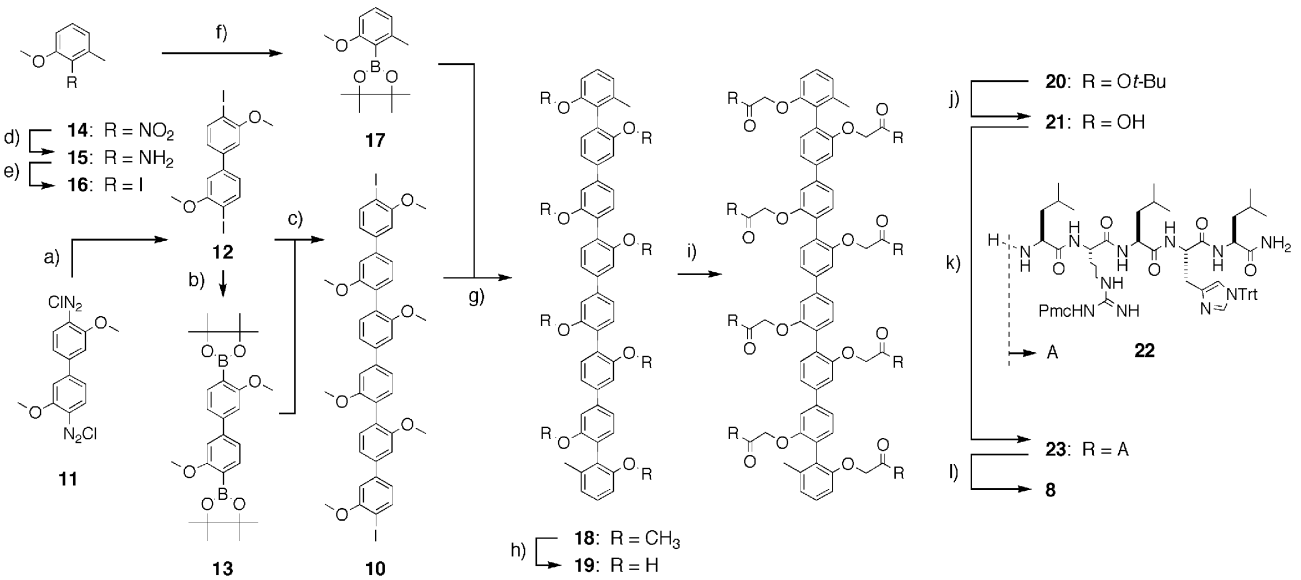

Scheme 1 (a) KI, 70%;[33] (b) 4,4,5,5-tetramethyl-[1,3,2]-dioxaborolane, $PdCl_2$(dppf), 70%;[33] (c) $Pd(PPh_3)_4$, Na_2CO_3, 10%;[33] (d) Pd/C, H_2, quant.;[34] (e) 1. $NaNO_2$, H_2SO_4, 2. KI, 71%;[34,35] (f) 4,4,5,5-tetramethyl-[1,3,2]-dioxaborolane, $PdCl_2$(dppf), TEA, CH_3CN, 85 °C, 2.5 h, not isolated; (g) $Pd(PPh_3)_4$, K_2CO_3, DMSO–H_2O 4 : 1, microwave, 150 °C, 15 min, 60%; (h) BBr_3, CH_2Cl_2, −78 °C to rt, 14 h; (i) Cs_2CO_3, DMF, 80 °C, 1 h, then *tert*-butyl bromoacetate, 60 °C, 3 h, 49% from **18**; (j) TFA, rt, 3 h; (k) **22**,[36] HATU, TEA, DMF, rt, 2.5 h, 16% from **20**; (l) TFA, rt, 2 h, quant.

identical behavior. The key characteristic in the mass spectra, that is the spontaneous counterion exchange from the expected TFA to the detected phosphates, was reproduced.[37] This unexpected observation was the key to understand the similarly unexpected low conductance and cation selectivity of pore **1** above pH 5 and marked the beginning of a general investigation of the contribution of counteranions to the functions of oligoarginines such as the cell-penetrating peptides in lipid bilayer membranes and live cells.[38,39]

The NMR tags produced the expected resonances in silent regions of the NMR spectrum of target rod **8** (Fig. 3). Namely, the electron-donating 1^6 and 8^6 methyls shifted the 1^5 and 8^5 hydrogens in the *ortho* and the 1^3 and 8^3 hydrogens in the *para* positions upfield to 6.5 and 6.3 ppm, respectively. Comparison of the integrals of these isolated *p*-octiphenyl signals with those of peptide resonances provided facile and clearcut experimental confirmation of MS results that rod **8** is defect-free (*i.e.*, the presence of eight pentapeptides per rod rather than seven plus a defect such as a methyl ester).

In all common NMR solvents, these signals were, however, as broad as all other signals. Below findings demonstrated that symmetry losses with chiral lateral substitution contributed to this signal broadening besides the known polymorphous self-assembly at the comparably high millimolar concentrations needed in NMR spectroscopy. Namely, denaturation with TFA resulted in the expected line-sharpening. However, apparent triplets rather than doublets were observed for the $1^5/8^5$ and the $1^3/8^3$ hydrogens under these extreme, denaturing conditions (Fig. 3). Moreover, the $1^6/8^6$ methyls appeared as an apparent doublet at 1.8 ppm. 2D NMR NOESY revealed that the found signal fine structure originated from two separate spin systems with the expected doublet multiplicities from ^3J couplings. This chemical non-identity of the two terminal arenes A and H demonstrated that the introduction of the chiral lateral pentapeptides results in the loss of the center of symmetry in *p*-octiphenyl **8**.

2.2 Activity of β-barrel pores with isomeric rigid *p*-octiphenyl staves

Synthetic multifunctional pores formed by rigid-rod β-barrels **1** with conventional $1^3,2^3,3^2,4^3,5^2,6^3,7^2,8^3$-staves have been characterized in detail in both spherical[36,40] and planar bilayer membranes.[37] The activity of the isomeric rigid-rod β-barrels **9** with the novel $1^2,2^2,3^3,4^2,5^3,6^2,7^3,8^2$-staves was determined in large unilamellar vesicles (LUVs) composed of egg yolk phosphatidylcholine (EYPC) and loaded with the fluorescent probe 8-amino-1,3,6-naphthalenetrisulfonate (ANTS) and the quencher *p*-xylenebis(pyridinium) bromide (DPX), *i.e.*, EYPC-LUVs⊃ANTS/DPX.[36,40] After addition of $1^2,2^2,3^3,4^2,5^3,6^2,7^3,8^2$-rod **8**, release of either fluorophore or quencher from EYPC-LUVs⊃ANTS/DPX was readily detectable as an increase of ANTS emission (Fig. 4A). For pores with an interior large enough to allow for efflux of organics like ANTS and DPX, the ANTS/DPX assay is, in our hands, the assay of choice to determine c_M and pH profiles because of its minimal dependence on pH and anion/cation selectivity. According to the ANTS/DPX assay, the activity of pores **9** increased with decreasing pH (Fig. 4B). The pH profiles of the isomeric pores **9** and **1**[40] were nearly identical. pH-gated pore opening has been interpreted previously with the ICR model, *i.e.*, maximal pore activity at intermediate internal charge repulsion (ICR).[41,42] Contributions from internal arginines to ICR are expected to be weak because of charge neutralization by counteranion scavenging. The observed pore opening below pH 6 is therefore thought to originate chiefly from the stabilization of the internal space of pores **9** and **1** by intermediate ICR between increasingly protonated histidine residues below their intrinsic $pK_a = 6.0$.

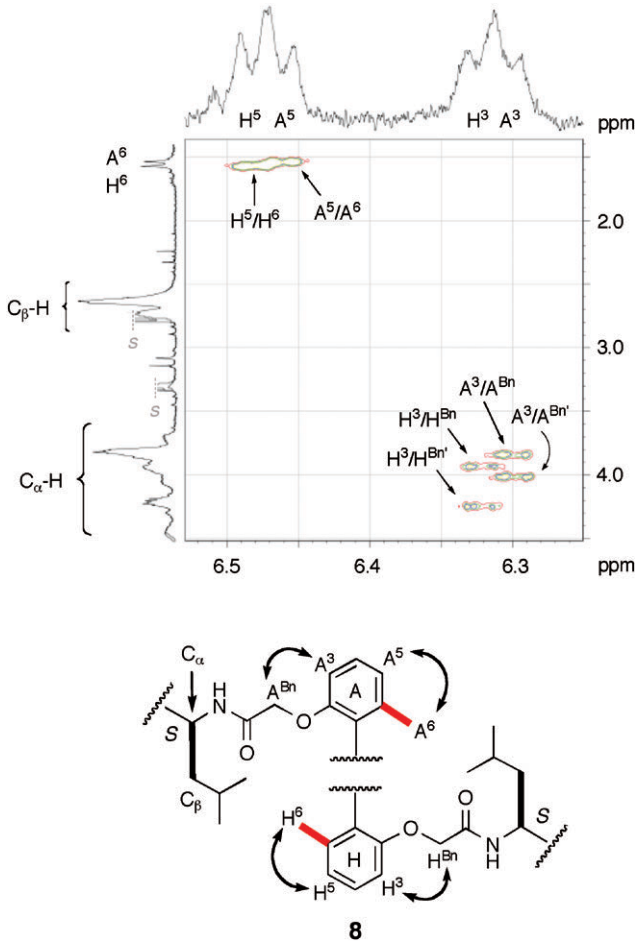

Fig. 3 Part of the 2D NOESY NMR spectrum of target molecule **8** in denaturing CF_3COOD–CD_3OD 3 : 1 (A and H indicate the non-identical terminal arenes 1 and 8, *s* = solvent).

Around optimal pH, the dependence of the activity of pores **9** in EYPC-LUVs⊃ANTS/DPX on the concentration c_M of monomeric rods **8** was nearly linear below the apparent half effective concentration EC50 under these conditions (Fig. 5A). A fit to the Hill equation for self-assembly >eqn (1)]:

$$\log Y = n \times \log c_M - n \times \log \mathrm{EC50} \qquad (1)$$

gave a Hill coefficient $n \approx 1$ (Y = fractional pore activity)[3]. As discussed elsewhere,[3] the interpretation of results from Hill analysis in the context of the self-assembly of functional supramolecules can be qualitatively classified into three categories:

$n > 1$ is observed with endergonic self-assembly of unstable functional supramolecules formed by n monomers,

$n \approx 1$ is observed with exergonic self-assembly of stable functional supramolecules (n is not indicative of the number of monomers per supramolecule),

$n < 1$ is observed with exergonic self-assembly of metastable functional supramolecules that transform into inactive higher assemblies at high concentration (*e.g.*, precipitate; n is not indicative of the number of monomers per supramolecule).

The found Hill coefficient $n \approx 1$, therefore, suggested that the self-assembly of pores **9** is exergonic under conditions

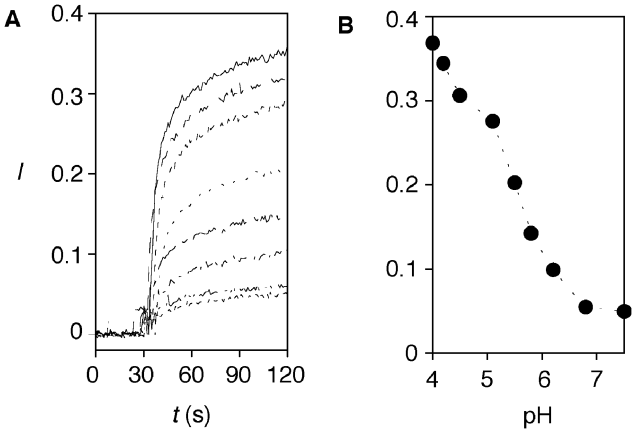

Fig. 4 pH profile of isomeric rigid-rod β-barrel pore **9** (B) with original traces (A) showing fractional change in ANTS emission I (λ_{ex} 360 nm, λ_{em} 520 nm) as a function of time during addition of rod **8** (final monomer concentration $c_M = 60$ nM; ≤15 nM tetrameric pores) to EYPC-LUVs⊃ANTS/DPX in buffer (~130 μM EYPC, 100 mM KCl, 10 mM MES) at, with decreasing activity, pH 4.2, 4.5, 5.1, 5.5, 5.8, 6.2, 6.8 and 7.5, calibrated by final lysis (excess triton X-100).

relevant for function. The apparent difference to $n < 1$ behavior of isomeric pore **1** ($n = 0.6$)[3,40] may suggest that the fibrillogenesis[43] of rigid-rod β-barrels with $1^3,2^3,3^2,4^3,5^2,6^3,7^2,8^3$-staves is hindered in isomeric rigid-rod β-barrels with $1^2,2^2,3^3,4^2,5^3,6^2,7^3,8^2$-staves. The apparent difference in the c_M profiles of pores **1** and **9** is, however, with all likelihood, of minor relevance because the differentiation between $n \approx 1$ and $n < 1$ behavior is often a question of subtle experimental conditions (*e.g.*, solvent and concentration of stock solutions). These reservations do not apply to the, in our experience, unambiguous differentiation of endergonic and exergonic self-assembly using $n > 1$ and $n \leq 1$ behavior.

The effective monomer concentration EC50, *i.e.*, the concentration where 50% pore activity is observed under given conditions, was EC50 = 90 nM. For a tetrameric pore **9**, this

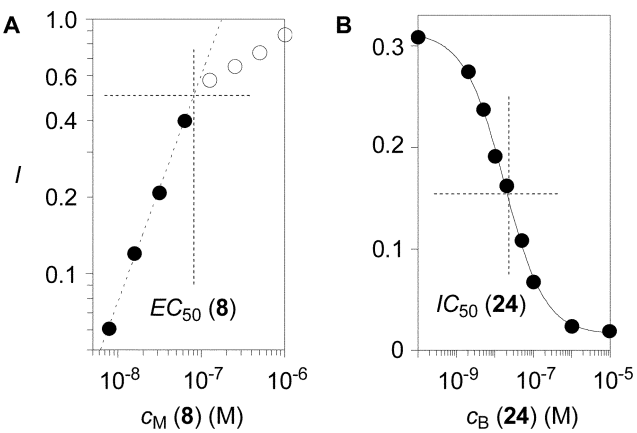

Fig. 5 Dependence of the fractional activity I of pore **9** on the concentration c_M of monomer **8** with linear curve fit below the effective concentration EC50 (c_M profile, A, pH 4.0) and the concentration c_B of poly(L-glutamic acid) blocker **24** [c_B profile, B, $c_M = 60$ nM (≤15 nM tetrameric pores), pH 4.5] with curve fit to Hill eqn (1); method and other conditions as in Fig. 3.

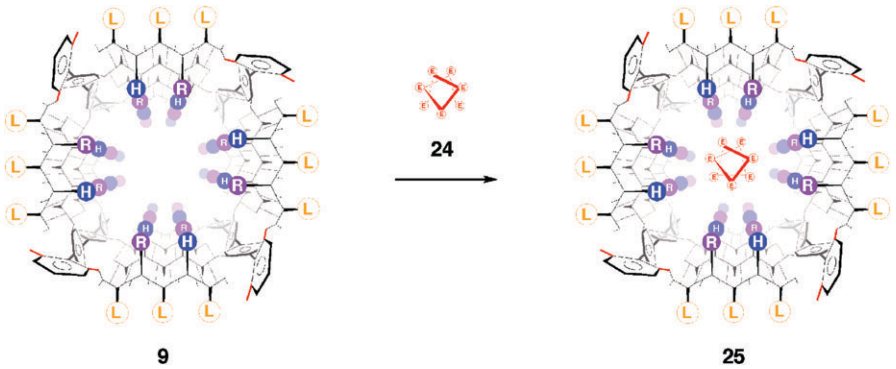

Fig. 6 Blockage of isomeric $1^2,2^2,3^3,4^2,5^3,6^2,7^3,8^2$-*p*-octiphenyl pores **9** by molecular recognition of α-helical poly(L-glutamic acid) **24** is expected to occur by formation of the supramolecular inclusion complex **25**.

was calculated to be a remarkable EC50 = 23 nM. This is the highest apparent activity observed for a rigid-rod β-barrel pore. Assessment of the EC50 of the isomeric pore **1** was not meaningful because of the onset of saturation below EC50 with $n \leq 1$ behavior.[40]

2.3 Multifunctionality of β-barrel pores with isomeric rigid *p*-octiphenyl staves

Molecular recognition by synthetic multifunctional pores **1–6** is attractive because host–guest chemistry within pores coincides with changes in pore activity and can therefore be controlled and detected by several attractive methods that are not available in isotropic media.[1,2] The recognition of α-helical guests turned out to be particularly attractive because the dimensions of the internal nanospaces of rigid-rod β-barrel pore hosts like **1** match those of, *e.g.*, α-helical poly(L-glutamic acid) **24** (Fig. 6).[1–4]

α-Helix recognition was, therefore, selected as an example of scientific relevance[44] to corroborate the functional similarity of the isomeric multifunctional pores **1** and **9**. To do so, the activity of synthetic multifunctional pore **9** in spherical EYPC-LUVs⊃ANTS/DPX was assessed in the presence of increasing concentrations of helix **24** at pH 4.5. As with isomer **1**,[15] the activity of pores **9** decreased with increasing concentrations of helix **24** (Fig. 5B). Fit of the obtained dose–response curve to the Hill equation for blockage [eqn (2)]:

$$\log Y = n \times \log c_B - n \times \log \mathrm{IC50} \qquad (2)$$

gave an inhibitory concentration IC50 = 12 ± 2 nM and a Hill coefficient $n = 0.8 \pm 0.1$. These results for blockage of pores **9** by α-helix recognition were similar to those obtained with isomeric pores **1**[36] and, therefore, suggestive of the formation of inclusion complex **25** (Fig. 6) with slightly negative cooperativity. The recent crystal structure of the translocator domain of the bacterial autotransporter NaIP from *Neisseria meningitidis* suggests that similar functional suprastructural architecture exists in nature.[45] Recent findings demonstrated that replacement not only of the biological β-barrel pore with synthetic multifunctional rigid-rod pores but also of that of the α-helix blocker with shape-persistent, supramolecular rigid-rod α-helix mimics is possible.[46]

The meaningfulness of an interpretation of the 10-times lower IC50 obtained for complex **25** compared to the isomeric complex with pore **1** as improved α-helix recognition with $1^2,2^2,3^3,4^2,5^3,6^2,7^3,8^2$-staves was questionable. Additional caution was indicated in comparisons of apparent IC50s near stoichiometric binding because they could, depending on experimental conditions, appear higher than they are in reality.[47]

2.4 Chirality of β-barrel pores with isomeric rigid *p*-octiphenyl staves

Denaturation experiments revealed that most monomeric *p*-oligophenyl staves are nearly CD silent.[48,49] This finding was in agreement with free atropisomerism around the arene–arene single bonds in monomeric rods **7** and **8**. The circular dichroism (CD) Cotton effects for the exciton-coupled low-energy L_a-transitions in the *p*-oligophenyl stave report, therefore, selectively on the supramolecular chirality of the self-assembled rigid-rod β-barrel. This supramolecular chirality is obviously induced by the stereogenic centers in the enantiopure pentapeptides. The CD spectrum of the regioisomeric, NMR-labelled $1^2,2^2,3^3,4^2,5^3,6^2,7^3,8^2$-rod **8** in bilayer membranes was nearly superimposable with that of the original $1^3,2^3,3^2,4^3,5^2,6^3,7^2,8^3$-rod **7** (Fig. 7). This similarity demonstrated that the supramolecular chirality of classical rigid-rod

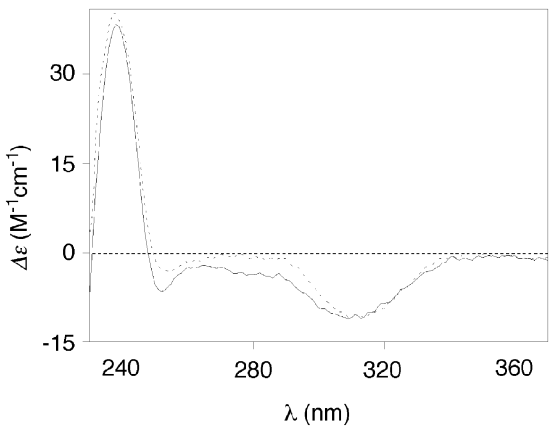

Fig. 7 Circular dichroism (CD) spectra of *p*-octiphenyls **7** (5 μM, dotted) and isomer **8** (5 μM, solid) in lipid bilayer membranes [EYPC-LUVs (250 μM EYPC), 100 mM KCl, 10 mM MES, pH 4.5].

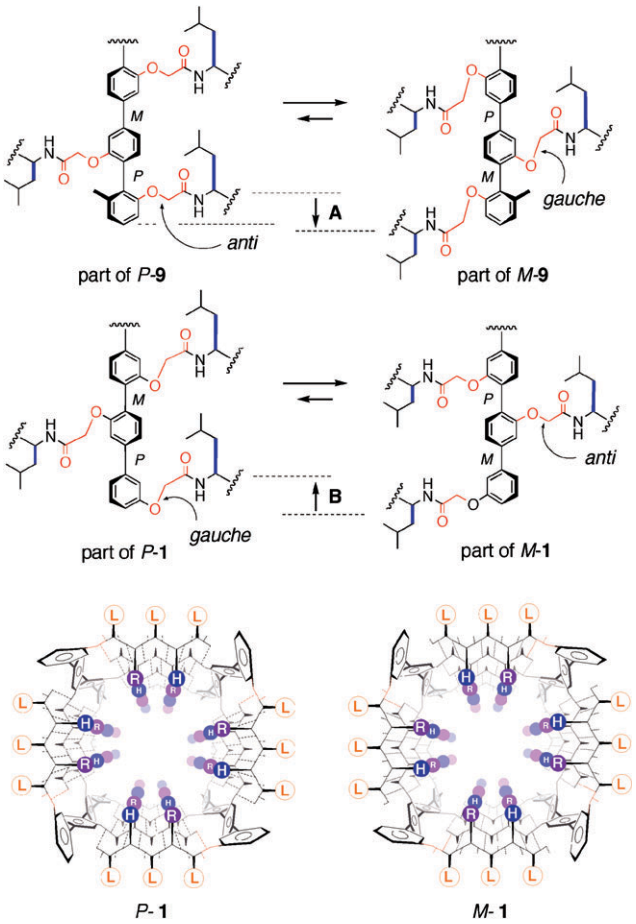

Fig. 8 Identical supramolecular barrel chirality with regioisomeric staves is proposed to originate from hoop–stave matching with expanded β-sheets (A) in *M*-supramolecules with glycolate spacers (red) in either *anti* (*M*-**1**) or *gauche* conformation (*M*-**9**, see Fig. 6).

β-barrel **1** and that of isomeric rigid-rod β-barrel **9** are identical (Fig. 2, 6 and 8).

This finding is not trivial. In rigid-rod β-barrels, the first and last amino-acid residues 1 and 5 of all pentapeptides are oriented to the outer barrel surface to avoid steric interference in the *p*-octiphenyl turns. With the given absolute pentapeptide chirality and glycolate spacers having C–O bonds in an *anti* conformation, this peripheral crowding enantioselectively freezes classical atropisomerizing *p*-octiphenyl staves in a zig-zag *M*,*P*,*M*,*P*,*M*,*P*,*M*-conformation. The resulting residual *M*-"helicity" of classical barrels like *M*-**1** has been verified in molecular mechanics simulations (Fig. 8).[3,4] In the isomeric $1^2,2^2,3^3,4^2,5^3,6^2,7^3,8^2$-stave **8**, the preserved pentapeptide chirality and an *anti* conformation of the glycolate spacers should induce the *P*,*M*,*P*,*M*,*P*,*M*,*P*-conformation of a barrel *P*-**9** with a mirror-imaged CD spectrum compared to *M*-**1**. The found identical CD spectra implied the stereoselective self-assembly of barrel *M*-**9** instead. This inversion of supramolecular chirality implied a conformational change in the lateral peptide strands. With inflexible β-sheets, rotation of the glycolate spacers from an *anti* conformation in *P*-**9** to a *gauche* in *M*-**9** remained as the only reasonable possibility for such a conformational change. The β-sheet expansion achieved by such an *anti* → *gauche* isomerization in *M*-**9** implied hoop–stave matching (rather than glycolate conformation) as the dominant driving force for the enantioselective self-assembly of *M*-barrels **1** and **9** (Fig. 8A). With classical barrels, the same *anti* → *gauche* isomerization is hindered by increasing hoop–stave mismatch with the β-sheet compression from the favored *M*-**1** to the unfavored *P*-**1** (Fig. 8B). Whatever the final suprastructural explanation will be, the bottom line at this stage is that the identical supramolecular chirality of regioisomeric barrels **1** and **9** implies conformational differences in the respective peptide hoops (*e.g.*, glycolate spacer) that occur for experimentally unverified reasons (*e.g.*, hoop–stave matching). The implied dependence of absolute barrel chirality on hoop conformation is in agreement with the well-documented sensitivity of supramolecular *p*-oligophenyl chirality to chemical modification, chemical stimulation, and heat.[50]

3 Conclusions

For reasons discussed elsewhere,[11,42,51,52] there is increasing awareness in the field that the most reliable insights on active suprastructures of synthetic and biological ion channels and pores may come from studies on function. According to this notion, we report that the self-assembly of rigid-rod β-barrels is roughly independent of the substitution pattern along the *p*-octiphenyl scaffold. Specifically, synthetic multifunctional pores formed by rigid-rod β-barrels with classical $1^3,2^3,3^2,4^3,5^2,6^3,7^2,8^3$-staves (*i.e.*, **7**) and regioisomeric $1^2,2^2,3^3,4^2,5^3,6^2,7^3,8^2$-staves (*i.e.*, **8**) have similar pH profiles, similar c_M profiles and exhibit similar dose–response curves for blockage by α-helical poly(L-glutamic acid). NMR tags added to the new stave **8** are found to facilitate the characterization of synthetic products and demonstrate the loss of central *p*-oligophenyl symmetry upon symmetric attachment of chiral substituents along the rigid-rod scaffold. Circular dichroism spectroscopy indicates that regioisomeric staves do not invert the absolute supramolecular chirality of the resulting barrel.

4 Experimental section

4.1 General

As in ref. 4. Reagents for synthesis, poly(glutamic acid) (*M* 13 600 g mol^{-1}), buffers and salts were from Sigma, Fluka, Aldrich or Acros, amino acid derivatives from Novabiochem, EYPC from Avanti, ANTS and DPX from Molecular Probes. Solvents were dried by use of a solvent purification system from Solv-tek. Microwave reactions were carried out using a Biotage Initiator™ microwave synthesizer. Column chromatography was carried out on silica gel 60 (Fluka, 40–63 μm). Sephadex LH-20 was from Amersham Biosciences. Analytical (TLC) and preparative thin layer chromatography (PTLC) were performed using silica gel 60 (Fluka, 0.2 mm) and silica gel GF (Analtech, 1000 μm), respectively. Purity of the products was confirmed by HPLC by using either Jasco HPLC system (PU-980, UV-970, FP-920) or Agilent 1100 Series. ESI-

MS was performed on either an Applied Biosystems API 150 Ex or a Finnigan MAT SSQ 7000 instrument. APCI-MS was performed using the latter instrument. ^{1}H and ^{13}C NMR spectra were recorded (as indicated) on either a DRX Bruker 300 MHz, 400 MHz or 500 MHz spectrometer and are reported as chemical shifts (δ) in ppm relative to TMS (δ = 0). Spin multiplicities are reported as singlet (s), doublet (d) or triplet (t), with coupling constants (J) given in Hz. The 500 MHz NOESY spectrum of **8** was acquired using a square window of 9.4 ppm. In the first dimension, 256 increments were acquired resulting in a resolution of 18.35 Hz per point. In the direct dimension, the number of time data points was 4k resulting in a digital resolution of 1.15 Hz per point. After processing using 512 × 8k points and no window function, cross peaks and diagonal signals had the same signs indicating an NOE in the slow motion regime. The mixing time was 500 ms and the recovery period 1.83 s. UV-Vis measurements were preformed on a Varian Cary 1 Bio spectrophotometer, CD measurements on a Jasco J-715 spectropolarimeter and fluorescence measurements were preformed on a Fluoro-Max-3, Jobin Yvon-Spex, equipped with an injector port, a stirrer and a temperature controller (25 °C). pH, c_M and c_B profiles of pore **9** were obtained as reported previously for pore **1**.[35,40,46]

4.2 Synthesis

2-Iodo-3-methylanisole (16). This compound was prepared in 2 steps from **14** following previously reported procedures.[34,35]

1^4,6^4-Diiodo-1^3,2^3,3^2,4^3,5^2,6^3-hexamethoxy-*p*-sexiphenyl (10). This compound was prepared in 3 steps from **11** following previously reported procedures.[33]

1^6,8^6-Dimethyl-1^2,2^2,3^3,4^2,5^3,6^2,7^3,8^2-octamethoxy-*p*-octiphenyl (18). To a solution of **16** (89 mg, 0.36 mmol) in degassed anhydrous acetonitrile (4 ml), were added $PdCl_2$(dppf) (10 mol%), TEA (300 µl, 2.16 mmol) and 4,4,5,5-tetramethyl-[1,3,2]-dioxaborolane (160 µl, 1.08 mmol) successively and the solution set to stir at 85 °C for 2.5 h. The reaction was cooled to room temperature and activated charcoal was added to the reaction mixture. The mixture was sonicated, filtered and the filtrate concentrated *in vacuo* to yield crude 2-(4,4,5,5-tetramethyl-[1,3,2]-dioxaborolane)-3-methylanisole **17**. To a 20 ml glass microwave vessel was added **10** (40 mg, 45 µmol) in DMF–H_2O (4 : 1) (10 ml). Following the addition of $Pd(PPh_3)_4$ (10 mol%), K_2CO_3 (37 mg, 0.27 mmol) and crude **17** obtained above (assumed 0.36 mmol), the solution was degassed and put under N_2. The reaction was microwaved at 150 °C while stirring during 15 min, cooled to room temperature, the product extracted into CH_2Cl_2 (15 ml), washed with brine (15 ml × 3) and concentrated *in vacuo*. Purification of the product first by column chromatography (CH_2Cl_2) and then by preparative thin layer chromatography (CH_2Cl_2–petroleum ether 10 : 1) gave **18** (24 mg, 60%) as a colorless solid. TLC (CH_2Cl_2–petroleum ether 10 : 1): R_f 0.44; ^{1}H NMR (400 MHz, $CDCl_3$): δ 7.43 (dd, ^4J = 2.3 Hz, ^3J = 7.6 Hz, 4H), 7.34–7.26 (m, 14H), 7.20 (d, ^3J = 7.6 Hz, 2H), 6.94 (d, ^3J = 7.6 Hz, 2H), 6.87 (d, ^3J = 8.1 Hz, 2H), 3.93 (s, 6H), 3.92 (s, 6H), 3.85 (s, 6H), 3.77 (s, 6H), 2.12 (s, 3H); ^{13}C NMR (100 MHz, $CDCl_3$): δ 157.5 (s, 8×), 142.4 (s, 2×), 142.3 (s, 2×), 142.0 (s, 2×), 138.8 (s, 2×), 132.1 (d, 2×), 132.0 (d, 2×), 131.9 (d, 2×), 128.3 (d, 2×), 127.3 (s, 2×), 126.8 (s, 2×), 126.6 (s, 2×), 125.9 (s, 2×), 122.5 (d, 2×), 119.7 (d, 4×), 119.6 (d, 2×), 110.6 (d, 2×), 110.5 (d, 2×), 110.4 (d, 2×), 108.7 (d, 2×), 56.2 (q, 2×), 56.1 (q, 4×), 56.0 (q, 2×), 20.3 (q, 2×); MS (APCI, CH_2Cl_2): m/z (%) 880 (100, $[M + H]^+$).

1^6,8^6-Dimethyl-1^2,2^2,3^3,4^2,5^3,6^2,7^3,8^2-octakis(*Gla*-O*t*Bu)-*p*-octiphenyl (20). To a solution of octaanisole **18** (24 mg, 27 µmol) in CH_2Cl_2 (5 ml), was added boron tribromide (0.7 ml, 1 M solution in CH_2Cl_2, 0.7 mmol) at −78 °C. The solution was allowed to warm to room temperature over 14 h, quenched with MeOH (1 ml) and then concentrated *in vacuo* to give crude octaphenol **19**. Crude **19** was dissolved in DMF (5 ml), treated with Cs_2CO_3 (211 mg, 0.65 mmol) at 80 °C for 1 h, and then with *tert*-butyl bromoacetate (96 µl, 0.65 mmol) at 60 °C for 3 h. The resulting suspension was diluted with CH_2Cl_2 (15 ml), washed with brine (20 ml × 3), dried over Na_2SO_4, and concentrated *in vacuo*. Flash column chromatography (CH_2Cl_2–MeOH 100 : 1) followed by PTLC (CH_2Cl_2–toluene–MeOH 7 : 3 : 0.1) gave pure **20** as a colorless solid (22 mg, 49%). TLC (CH_2Cl_2–toluene–MeOH 7 : 3 : 0.1): R_f 0.69; ^{1}H NMR (400 MHz, $CDCl_3$): δ 7.54 (dd, ^4J = 3.0 Hz, ^3J = 7.8 Hz, 4H), 7.33–7.29 (m, 8H), 7.22 (t, ^3J = 8.0 Hz, 2H), 7.13 (s, 4H), 7.10 (s, 2H), 6.96 (d, ^3J = 7.6 Hz, 2H), 6.72 (d, ^3J = 8.3 Hz, 2H), 4.59 (s, 8H), 4.50 (s, 4H), 4.45 (s, 4H), 1.49 (s, 18H), 1.48 (s, 18H), 1.47 (s, 18H), 1.45 (s, 18H); ^{13}C NMR (100 MHz, $CDCl_3$): δ 168.6 (s, 2×), 168.5 (s, 2×), 168.3 (s, 4×), 156.1 (s, 2×), 156.0 (s, 2×), 155.9 (s, 4×), 141.9 (s, 2×), 141.8 (s, 2×), 141.5 (s, 2×), 139.4 (s, 2×), 132.6 (d, 2×), 132.5 (d, 2×), 132.4 (d, 2×), 128.2 (d, 2×), 127.4 (s, 2×), 126.8 (s, 2×), 126.6 (s, 2×), 126.2 (s, 2×), 123.4 (d, 2×), 120.5 (d, 2×), 120.4 (d, 2×), 120.3 (d, 2×), 111.7 (d, 4×), 111.6 (d, 2×), 109.8 (d, 2×), 82.2 (s, 4×), 82.1 (s, 2×), 82.0 (s, 2×), 66.8 (t, 8×), 28.3 (q, 4×), 28.2 (q, 2×), 28.2 (q, 2×), 20.5 (q, 2×); MS (ESI, CH_2Cl_2–MeOH 9 : 1): m/z (%) 1698 (100, $[M + H_3O]^+$), 858 (40, $[M + H + H_3O]^{2+}$).

1^6,8^6-Dimethyl-1^2,2^2,3^3,4^2,5^3,6^2,7^3,8^2-octakis(*Gla*-OH)-*p*-octiphenyl (21). To **20** (11 mg, 6.5 µmol) was added TFA (1 ml) and the solution was allowed to stir for 1 h 30 min, after which toluene (1 ml) was added and the solution concentrated *in vacuo*. The product was washed with hexane (1 ml × 3), following which TFA (1 ml) was again added and the solution allowed to stir for an additional 1 h 30 min. Toluene (1 ml) was added, the solution concentrated *in vacuo*, washed with hexane (1 ml × 3) and dried to give **21** (8 mg, quant.) as a colorless solid. ^{1}H NMR (300 MHz, CD_3OD): δ 7.46 (d, ^3J = 7.6 Hz, 4H), 7.36 (d, ^3J = 8.0 Hz, 6H), 7.29–7.18 (m, 10H), 6.95 (d, ^3J = 7.5 Hz, 2H), 6.80 (d, ^3J = 8.3 Hz, 2H), 4.74 (s, 8H, CH_2), 4.64 (s, 4H), 4.56 (s, 4H), 2.14 (s, 6H); MS (ESI, CH_2Cl_2–MeOH 50 : 1): m/z (%) 1254 (61, $[M + Na]^+$), 1249 (100, $[M + H_3O]^+$), 1232 (24, $[M + H]^+$).

Leu-Arg(Pmc)-Leu-His(Trt)-Leu-NH$_2$ (22). This compound was prepared in 8 steps following previously reported procedures.[36]

$1^6,8^6$-Dimethyl-$1^2,2^2,3^3,4^2,5^3,6^2,7^3,8^2$-octakis[*Gla*-Leu-Arg(Pmc)-Leu-His(Trt)-Leu-NH_2]-*p*-octiphenyl (23). TEA (43 μl, 0.31 mmol) was added to a DMF (1 ml) solution containing **21** (8 mg, 6.5 μmol), **22** (84 mg, 73 μmol) and HATU (28 mg, 73 μmol). The reaction was allowed to stir at room temperature for 2 h 30 min, before being concentrated *in vacuo*. Flash column chromatography (CH_2Cl_2–MeOH 4 : 1), followed by size exclusion chromatography (Sephadex LH-20, MeOH) and then PTLC ($CHCl_3$–MeOH 9 : 1) gave **23** as a colorless solid (11 mg, 16%). HPLC (YMC-Pack silica, 250 × 10 mm, CH_2Cl_2–MeOH 90 : 10, 2 ml min^{-1}, t_R = 6.55 min); ^1H NMR (400 MHz, $CDCl_3$–CD_3OD 4 : 1): δ 7.57–6.91 (several m, 148H), 6.81–6.66 (several m, 10H), 5.07–4.31 (several m, 56H), 3.25–2.77 (several m, 32H), 2.6–2.35 (m, 64H), 2.10–1.98 (several m, 30H), 1.83–1.08 (several m, 168H), 0.93–0.49 (m, 144H); MS (ESI, [CH_3CN–H_2O–AcOH 74 : 24 : 2]–[MeOH] 9 : 1): *m*/*z* (%) 2589 (100, $[M + 4H]^{4+}$), 2529 (85, $[M + 4H - Trt]^{4+}$), 2468 (15, $[M + 4H - 2Trt]^{4+}$), 2072 (10, $[M + 5H]^{5+}$).

$1^6,8^6$-Dimethyl-$1^2,2^2,3^3,4^2,5^3,6^2,7^3,8^2$-octakis(*Gla*-Leu-Arg-Leu-His-Leu-NH_2)-*p*-octiphenyl (8). Compound **23** (11 mg, 1 μmol) was dissolved in TFA (1 ml). After stirring for 1 h at room temperature toluene (1 ml) was added and the reaction mixture concentrated *in vacuo*. The product was washed with hexane (1 ml × 3), following which TFA (1 ml) was again added and the solution allowed to stir for 1 h. Toluene (1 ml) was added and the product concentrated *in vacuo*. The product was dissolved in methanol and impurities were removed by extracting with hexane (1 ml × 3) to give **8** as a colorless solid (7 mg, quant.). RP HPLC (YMC-Pack ODS-A, 250 × 10 mm, [MeOH + 1% TFA]–[H_2O + 1% TFA] 85 : 15, 2 ml min^{-1}, t_R = 5.93 min); ^1H NMR (500 MHz, CF_3COOD–CD_3OD 3 : 1): δ 7.14–6.56 (several m, 36H), 6.48 (d, ^3J = 8.2, 1H), 6.46 (d, ^3J = 8.0, 1H), 6.32 (d, ^3J = 7.9, 1H), 6.30 (d, ^3J = 7.4, 1H), 4.50–3.65 (several m, 56H), 2.73–2.52 (several m, 32H), 1.57 (s, 3H), 1.54 (s, 3H), 1.33–0.55 (several m, 104H), 0.42–0.01 (m, 144H); MS (ESI, [CH_3CN–H_2O–AcOH 74 : 24 : 2]–[MeOH] 9 : 1): *m*/*z* (%) 1297 (15, $[M + 2H_3PO_4 + 5H]^{5+}$), 1277 (9, $[M + 1H_3PO_4 + 5H]^{5+}$), 1258 (2, $[M + 5H]^{5+}$), 1066 (15, $[M + 1H_3PO_4 + 6H]^{6+}$), 1049 (3, $[M + 6H]^{6+}$), 899 (100, $[M + 7H]^{7+}$), 913 (37, $[M + 1H_3PO_4 + 8H]^{8+}$), 908 (40, $[M + 1AcOH + 8H]^{8+}$), 787 (15, $[M + 8H]^{8+}$).

Acknowledgements

We thank M. Juillard for assistance in organic synthesis, P. Perrottet and the group of F. Gülaçar for MS measurements, and the Swiss NSF for financial support (including the National Research Program "Supramolecular Functional Materials" 4047–057496).

References

1 N. Sakai, J. Mareda and S. Matile, *Acc. Chem. Res.*, 2005, **38**, 79–87.
2 N. Sakai and S. Matile, *Chem. Commun.*, 2003, 2514–2523.
3 S. Litvinchuk, G. Bollot, J. Mareda, A. Som, D. Ronan, M. R. Shah, P. Perrottet, N. Sakai and S. Matile, *J. Am. Chem. Soc.*, 2004, **126**, 10067–10075.
4 V. Gorteau, F. Perret, G. Bollot, J. Mareda, A. N. Lazar, A. W. Coleman, D.-H. Tran, N. Sakai and S. Matile, *J. Am. Chem. Soc.*, 2004, **126**, 13592–13593.
5 J. Kumaki, E. Yashima, G. Bollot, J. Mareda, S. Litvinchuk and S. Matile, *Angew. Chem., Int. Ed.*, 2005, **44**, 6154–6157.
6 G. Das, P. Talukdar and S. Matile, *Science*, 2002, **298**, 1600–1602.
7 N. Sordé, G. Das and S. Matile, *Proc. Natl. Acad. Sci. USA*, 2003, **100**, 11964–11969.
8 S. Litvinchuk, N. Sordé and S. Matile, *J. Am. Chem. Soc.*, 2005, **127**, 9316–9317.
9 N. Sakai, N. Sordé and S. Matile, *J. Am. Chem. Soc.*, 2003, **125**, 7776–7777.
10 R. S. Hector and M. S. Gin, *Supramol. Chem.*, 2005, **17**, 129–134.
11 S. Matile, A. Som and N. Sordé, *Tetrahedron*, 2004, **60**, 6405–6435.
12 K. D. D. Mitchell and T. M. Fyles, in *Encyclopedia of Supramolecular Chemistry*, ed. J. L. Atwood and J. W. Steed, Marcel Dekker, New York, 2004, pp. 742–746.
13 U. Koert, *Bioorg. Med. Chem.*, 2004, **12**, 1277–1350.
14 U. Koert, L. Al-Momani and J. R. Pfeifer, *Synthesis*, 20048), 1129.
15 J. M. Boon and B. D. Smith, *Curr. Opin. Chem. Biol.*, 2002, **6**, 749–756.
16 G. W. Gokel and A. Mukhopadhyay, *Chem. Soc. Rev.*, 2001, **30**, 274–286.
17 G. J. Kirkovits and C. D. Hall, *Adv. Supramol. Chem.*, 2000, **7**, 1–47.
18 P. Scrimin and P. Tecilla, *Curr. Opin. Chem. Biol.*, 1999, **3**, 730–735.
19 W. H. Chen and S. L. Regen, *J. Am. Chem. Soc.*, 2005, **127**, 6538–6539.
20 W.-Y. Yang, J.-H. Ahn, Y.-S. Yoo, N.-K. Oh and M. Lee, *Nat. Mater.*, 2005, **4**, 399–402.
21 M. Yoshii, M. Yamamura, A. Satake and Y. Kobuke, *Org. Biomol. Chem.*, 2004, **2**, 2619–2623.
22 Y. J. Jeon, H. Kim, S. Jon, N. Selvapalam, D. H. Oh, I. Seo, C.-S. Park, S. R. Jung, D.-S. Koh and K. Kim, *J. Am. Chem. Soc.*, 2004, **126**, 15944–15945.
23 V. Percec, A. E. Dulcey, V. S. Balagurusamy, Y. Miura, J. Smidrkal, M. Peterca, S. Nummelin, U. Edlund, S. D. Hudson, P. A. Heiney, H. Duan, S. N. Magonov and S. A. Vinogradov, *Nature*, 2004, **430**, 764–768.
24 V. Sidorov, F. W. Kotch, J. L. Kuebler, Y.-F. Lam and J. T. Davis, *J. Am. Chem. Soc.*, 2003, **125**, 2840–2841.
25 A. V. Koulov, T. N. Lambert, R. Shukla, M. Jain, J. M. Boon, B. D. Smith, H. Li, D. N. Sheppard, J.-B. Joos, J. P. Clare and A. P. Davis, *Angew. Chem., Int. Ed.*, 2003, **42**, 4931–4933.
26 Y. R. Vandenburg, B. D. Smith, E. Biron and N. Voyer, *Chem. Commun.*, 2002, 1694–1695.
27 J. M. Sanderson and S. Yazdani, *Chem. Commun.*, 2002, 1154–1155.
28 F. De Riccardis, M. Di Filippo, D. Garrisi, I. Izzo, F. Mancin, L. Pasquato, P. Scrimin and P. Tecilla, *Chem. Commun.*, 2002, 3066–3067.
29 J. Sanchez-Quesada, M. P. Isler and M. R. Ghadiri, *J. Am. Chem. Soc.*, 2002, **124**, 10004–10005.
30 D. Wang, L. Guo, J. Zhang, L. R. Jones, Z. Chen, C. Pritchard and R. W. C. Roeske, *J. Pept. Res.*, 2001, **57**, 301–306.
31 H. Ishida, Z. Qi, M. Sokabe, K. Donowaki and Y. Inoue, *J. Org. Chem.*, 2001, **66**, 2978–2989.
32 C. Pérez, C. G. Espínola, C. Foces-Foces, P. Núñez-Coello, H. Carrasco and J. D. Martín, *Org. Lett.*, 2000, **2**, 1185–1188.
33 N. Sakai, D. Gerard and S. Matile, *J. Am. Chem. Soc.*, 2001, **123**, 2517–2524.
34 R. S. Coleman, J. M. Guernon and J. T. Roland, *Org. Lett.*, 2000, **2**, 277.
35 S. M. Kerwin and M. M. McPhee, *US Patent* 155443, 2002.
36 N. Sordé and S. Matile, *J. Supramol. Chem.*, 2002, **2**, 191–199.
37 N. Sakai, N. Sordé, G. Das, P. Perrottet, D. Gerard and S. Matile, *Org. Biomol. Chem.*, 2003, **1**, 1226–1231.
38 N. Sakai and S. Matile, *J. Am. Chem. Soc.*, 2003, **125**, 14348–14356.
39 F. Perret, M. Nishihara, T. Takeuchi, S. Futaki, A. N. Lazar, A. W. Coleman, N. Sakai and S. Matile, *J. Am. Chem. Soc.*, 2005, **127**, 1114–1115.
40 P. Talukdar, N. Sakai, N. Sordé, D. Gerard, V. M. F. Cardona and S. Matile, *Bioorg. Med. Chem.*, 2004, **12**, 1325–1336.

41 B. Baumeister, A. Som, G. Das, N. Sakai, F. Vilbois, D. Gerard, S. P. Shahi and S. Matile, *Helv. Chim. Acta*, 2002, **85**, 2740–2753.
42 A. Som and S. Matile, *Chem. Biodiversity*, 2005, **2**, 717–729.
43 G. Das, L. Ouali, M. Adrian, B. Baumeister, K. J. Wilkinson and S. Matile, *Angew. Chem., Int. Ed.*, 2001, **40**, 4657–4661.
44 M. W. Peczuh and A. D. Hamilton, *Chem. Rev.*, 2000, **100**, 2479–2494.
45 C. J. Oomen, P. van Ulsen, P. van Gelder, M. Feijen, J. Tommassen and P. Gros, *EMBO J.*, 2004, **23**, 1257–1266.
46 S. Litvinchuk and S. Matile, *Supramol. Chem.*, 2005, **17**, 135–139.
47 O. H. Straus and A. Goldstein, *J. Gen. Physiol.*, 1943, **26**, 559–585.
48 G. Das, N. Sakai and S. Matile, *Chirality*, 2002, **14**, 18–24.
49 G. Das and S. Matile, *Chirality*, 2001, **13**, 170–176.
50 N. Sakai and S. Matile, *Chirality*, 2004, **16**, S28–S35.
51 Y. Baudry, G. Bollot, V. Gorteau, S. Litvinchuk, J. Mareda, M. Nishihara, D. Pasini, F. Perret, D. Ronan, N. Sakai, M. R. Shah, A. Som, N. Sordé, P. Talukdar, D.-H. Tran and S. Matile, *Adv. Funct. Mater*.DOI: 10.1002/adfm.200500198.
52 The State of Ion Channel Research in 2004, *Nat. Rev. Drug Discovery*, 2004, **3**, 239–278.

